



In-vivo safety evaluation of drug loaded hydrogel implant delivery system in orthotopic triple-negative breast cancer model

Lenkaphothula Naresh Goud^{1,2} and G.S. Vinod Kumar^{1*}

¹Nano Drug Delivery Systems (NDDS), Cancer Biology Division, Rajiv Gandhi Centre for Biotechnology (BRIC-RGCB), Thiruvananthapuram-695014, Kerala, India. ²Regional Centre for Biotechnology (BRIC-RCB), Faridabad, Haryana-121001, India.

Citation: Naresh Goud L, Vinod Kumar G.S .2025. In-vivo safety evaluation of drug loaded hydrogel implant delivery system in orthotopic triple negative breast cancer model. *J. Vet. Anim. Sci.* **56** (4): 723-729

Received: 09.12.2025

Accepted: 16.12.2025

Published: 31.12.2025

Abstract

Triple-negative breast cancer (TNBC) is commonly treated with systemic chemotherapy, which often results in dose-limiting off-target toxicity. In the present study, we evaluated the in-vivo safety of an injectable, drug-loaded hydrogel implant designed for localized and sustained intratumoral chemotherapy delivery in an orthotopic TNBC mouse model. Female NOD-SCID mice bearing MDA-MB-231 tumours were treated with either blank hydrogel, free chemotherapeutic drugs administered via tail vein, or intratumoral injection of the drug-loaded hydrogel. Eight weeks post-treatment, major organs including the heart, liver, lungs, kidneys, spleen, brain, ovaries, and urinary bladder were harvested and subjected to histopathological evaluation using haematoxylin and eosin staining. Systemic administration of free drugs resulted in marked architectural damage in multiple organs, including cardiomyocyte disorganization, renal glomerular damage, splenic structural disruption, ovarian follicular depletion, and bladder wall degeneration. In contrast, mice treated with the intratumoral drug-loaded hydrogel exhibited well-preserved tissue architecture across all examined organs, comparable to control and blank hydrogel groups. These findings demonstrate that localized intratumoral delivery of chemotherapeutic agents via hydrogel significantly reduces systemic toxicity while preserving normal organ morphology, highlighting its potential as a safer localized drug delivery platform for TNBC.

Keywords: Chemotherapy, toxicity, localized drug delivery

Breast cancer is currently the most common cancer globally, accounting for 12.5% of all new annual cancer cases worldwide. It is the commonest malignancy among women globally. It has now surpassed lung cancer as the leading cause of global cancer incidence in 2020, with an estimated 2.3 million new cases and 685000 deaths globally (Sung et al., 2021). Triple-negative breast cancer (TNBC), which accounts for 15–20% of incident breast cancers, is the only breast cancer subtype that lacks targeted treatments (Zagami et al., 2022). Chemotherapy is one of the most common cancer treatments in clinics. In most cases, the clinical responses show that the efficacy of chemotherapy is limited by the development of multi drug resistance (MDR) in cancer cells during a long period of treatment. To overcome the resistance, higher dose of toxic anticancer drugs is sometimes required, which kill healthy cells and result in adverse side effects. Treatment of common solid tumours has to be given as smaller doses placed out in cycles, to give healthy cells

*Corresponding author : G. S. Vinod Kumar, gsvinod@rgcb.res.in, Ph. 6238013720

time to recover in the intervals. But the drawbacks are that this approach may not kill all the cancer cells, and those that survive can become resistant to subsequent cycles of chemotherapy. Local therapy using novel drug delivery systems such as implanted devices or nanocarriers overcomes this limitation by continuously releasing drug providing sustained action at the tumour site by increasing dose intensity (Myung et al., 2024).

In this *in-vivo* safety evaluation model we injected a hydrogel loaded with chemotherapeutic drug intratumorally for site specific and sustained delivery of drugs to the tumour tissue. The developed drug delivery implant system preserves all the major organs architecture when compared to the tail vein injection group resulting in successful minimization of the off-target effects of the chemotherapy providing a safe non-invasive localized drug delivery system.

Materials and methods

The triple-negative breast cancer cell line MDA-MB-231 was obtained from the institutional cell repository, Rajiv Gandhi Centre for Biotechnology (RGCB). All cells were cultured in Dulbecco's Modified Eagle Medium (DMEM) supplemented with 10 per cent FBS and 1 per cent antibiotics. Female NOD SCID mice (4-6 weeks) were maintained in Animal research facility, RGCB and housed in cages. All *in vivo* experiments performed were approved by the Institutional Animal Ethical Committee (IAEC) under the protocol number IAEC/983/GSV/2024.

A total of 5×10^6 MDA-MB-231 cells were orthotopically injected into the mammary fat pad of female NOD-SCID mice of 4-6 weeks. When the tumour volume reached 75-100 mm³, the mice were randomly grouped into four groups (n=5), control, blank hydrogel, free drugs via tail vein and intra tumoral hydrogel (Hydrogel loaded with doxorubicin, cyclophosphamide and paclitaxel). The tail vein free drug group received systemic chemotherapy consisting of doxorubicin (7.5 mg/kg) and cyclophosphamide (75 mg/kg) administered via tail vein on day 1, followed by paclitaxel (10 mg/kg) administered via tail vein on day 7. This treatment cycle was repeated weekly for a total duration of 7 weeks. In contrast, the intratumoral hydrogel group received a single intratumoral injection of hydrogel loaded with equivalent doses of doxorubicin, cyclophosphamide, and paclitaxel, administered only on day 1. No additional dosing was performed in the intratumoral hydrogel group during the study period. This dosing strategy was designed to compare repeated systemic exposure with a single localized sustained-release administration. On the 8th week of treatment, the mice were sacrificed, and the brain, heart, kidneys, liver, lungs, ovaries, urinary bladder and spleen of each mouse were isolated. The tissues isolated from mice were fixed in 4 per cent neutral buffered formalin for 48 h and embedded in paraffin blocks. The embedded

tissues were cut into ~5 μ m sections for Hematoxylin & Eosin (H & E) staining (Cardiff et al., 2014). H & E-stained were observed and imaged under an optical microscope.

Results and Discussion

Systemic administration of chemotherapeutic agents is frequently associated with off-target toxicity affecting multiple non-tumour organs. Gross examination of tumoral tissues revealed marked differences among the treatment groups. The control, blank hydrogel, and free drug groups exhibited large, irregularly shaped tumours with substantial tumour mass, indicating progressive tumour growth and local invasion. In contrast, the intratumoral hydrogel group displayed a noticeably smaller and less vascularized tumour mass, suggesting effective inhibition of tumour growth following intratumoral administration of the drug-loaded hydrogel. While complete tumour remission was not observed, the reduced tumour size and vascularity indicate a strong local therapeutic response achieved through sustained intratumoral drug delivery.

Histopathological evaluation of vital tissues therefore provides critical insight into treatment-associated systemic damage and tissue preservation. Histopathological examination of urinary bladder tissue revealed distinct differences among the treatment groups (Fig. 1A-D). In the control and blank hydrogel groups, the urothelial architecture was largely preserved, although clusters of infiltrating cells were observed within the lamina propria. In the tail vein free drug group, severe architectural disruption of the bladder wall was evident, including loss of normal urothelial layering and increased stromal fibrosis. In contrast, the intratumoral hydrogel-treated group exhibited intact urothelial and submucosal architecture with no evidence of structural compromise. These findings are consistent with previous reports describing chemotherapy-induced bladder injury following systemic drug administration (Ritchey et al., 2009; Radswiki et al., 2025), while localized drug delivery approaches have been shown to reduce off-target urogenital toxicity.

Histological analysis of cardiac tissue revealed normal myocardial architecture in the control and blank hydrogel groups, characterized by well-aligned cardiomyocytes with intact striations (Fig. 1E-H). In contrast, the tail vein free drug group showed pronounced myocardial damage, including disrupted cardiac myofibers, loss of normal alignment, and widening of inter-fiber spaces. These changes are indicative of cardiotoxicity following repeated systemic exposure to paclitaxel, cyclophosphamide, and doxorubicin. Notably, cardiac tissue from the intratumoral hydrogel-treated group exhibited preserved myocardial structure comparable to controls, with no evident pathological alterations. These findings align with well-documented reports of chemotherapy-induced cardiotoxicity, particularly associated with

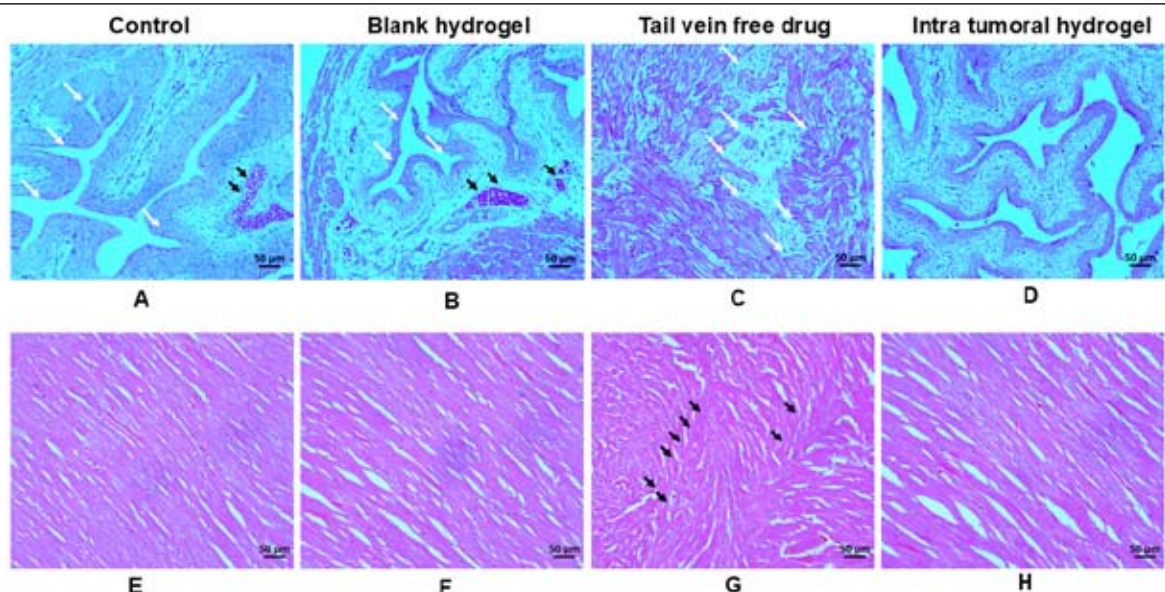


Fig. 1. Histopathological evaluation of urinary bladder and cardiac tissues.

(A–D): Urinary bladder. Control (A) and blank hydrogel (B) groups show relatively disrupted bladder wall architecture (white arrow) with focal cellular infiltration (black arrow). The free drug administered via tail vein group (C) exhibits marked urothelial disruption (white arrow). In contrast, the intratumoral hydrogel-treated group (D) shows intact urothelial lining and preserved submucosal architecture with minimal cellular infiltration. **(E–H): Cardiac tissue.** Control (E) and blank hydrogel (F) groups demonstrate well-organized myocardial fibers with intact striations. The tail vein free drug group (G) shows disrupted cardiac myofibers and loss of normal alignment (black arrow), indicative of chemotherapy-induced cardiotoxicity. The intratumoral hydrogel-treated group (H) exhibits preserved myocardial architecture comparable to controls. Hematoxylin and eosin staining; scale bar = 50 μ m.

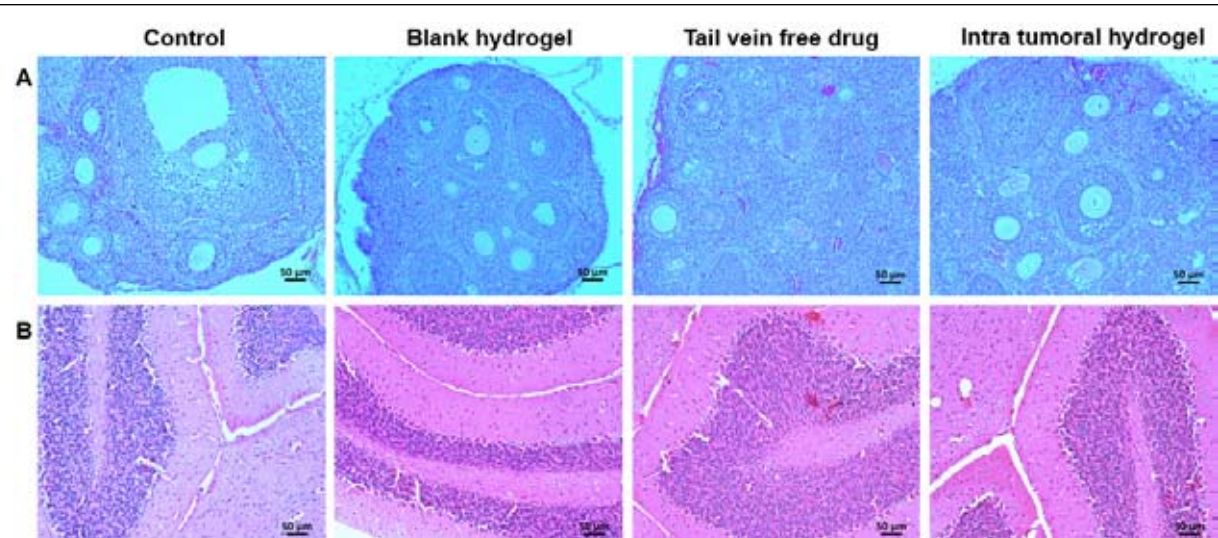


Fig. 2. Histopathological evaluation of ovarian and brain tissue.

(A): Ovary. Ovarian sections from the control and blank hydrogel groups show normal follicular architecture with the presence of primordial, primary, and antral follicles and intact ovarian stroma. In the tail vein free drug group, ovarian tissue exhibits marked follicular depletion, disrupted follicular organization, and reduced density of growing follicles, indicative of chemotherapy-induced ovarian toxicity. In contrast, the intratumoral hydrogel-treated group displays well-preserved follicular structures with minimal follicular loss, suggesting protection of ovarian tissue following localized drug delivery. **(B): Brain (cerebellum).** Cerebellar sections from all experimental groups, including control, blank hydrogel, tail vein free drug, and intratumoral hydrogel-treated mice, exhibit preserved neuronal architecture with intact cerebellar layers and no detectable histopathological alterations. Hematoxylin and eosin staining; scale bar = 50 μ m.

doxorubicin and paclitaxel, which can cause myocardial fiber disorganization, oxidative stress, and structural degeneration following systemic administration (Florescu

et al., 2013; Chen et al., 2024). The absence of such pathological features in the intratumoral hydrogel group reinforces previous evidence that localized chemotherapy

delivery reduces cardiac exposure and mitigates off-target cardiotoxic effects.

Histopathological evaluation of ovarian tissue revealed marked differences among treatment groups (Fig. 2A). The control and blank hydrogel groups exhibited normal ovarian morphology with well-preserved follicular architecture, including the presence of primordial, primary, and antral follicles. The ovarian stroma appeared dense and healthy, with no evidence of follicular atresia or degeneration. In contrast, the tail vein free drug group demonstrated pronounced ovarian damage, characterized by follicular depletion, disrupted follicular structure, and a reduced density of growing follicles. These findings indicate severe ovarian toxicity following repeated systemic chemotherapy. Notably, ovaries from the intratumoral hydrogel-treated group showed largely preserved follicular architecture with clear follicular boundaries and minimal follicular loss, suggesting protection of ovarian tissue following localized drug delivery.

The ovarian damage observed in the tail vein free drug group is consistent with well-documented cyclophosphamide-induced ovarian toxicity, attributed to its alkylating nature that causes DNA damage in actively growing follicles, leading to follicular depletion, premature ovarian failure, and infertility (Spears et al., 2019). Systemic exposure to combination chemotherapy regimens containing cyclophosphamide has been widely reported to

compromise ovarian reserve. In contrast, the preservation of ovarian architecture in the intratumoral hydrogel group supports previous evidence that localized chemotherapy delivery significantly reduces systemic drug exposure and spares reproductive organs from off-target toxicity.

Histopathological examination of brain tissue revealed no observable structural alterations across any of the treatment groups (Fig. 2B). The control, blank hydrogel, tail vein free drug, and intratumoral hydrogel-treated groups all exhibited well-preserved neuronal architecture with intact cellular organization and normal tissue morphology. No evidence of neuronal degeneration, inflammatory infiltration, or disruption of brain tissue architecture was detected in any group. These observations are consistent with previous reports indicating that conventional chemotherapeutic agents such as paclitaxel, cyclophosphamide, and doxorubicin generally exhibit limited penetration across the blood-brain barrier, thereby reducing the likelihood of overt histopathological damage in brain tissue (Bruna et al., 2020; Lehmann et al., 2020). The absence of detectable brain toxicity in the present study further supports the notion that both systemic and localized chemotherapy regimens used here did not induce measurable structural alterations in central nervous system tissue under the experimental conditions.

Histopathological examination of spleen sections revealed marked differences among treatment groups

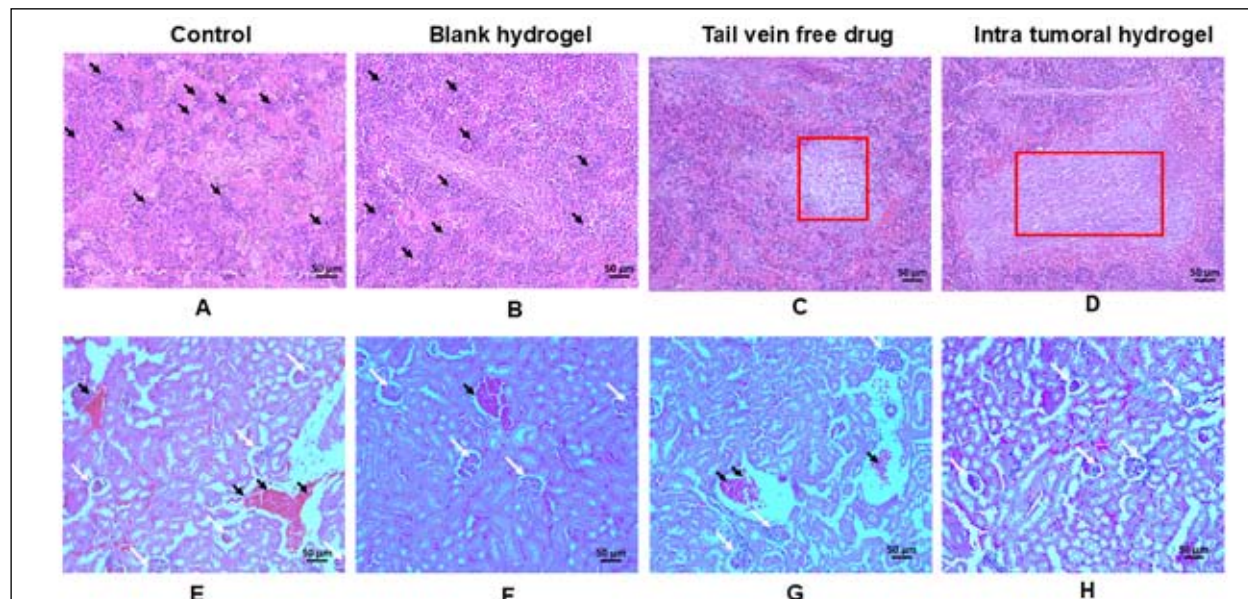


Fig. 3. Histopathological evaluation of spleen and kidney tissues.

(A-D): Spleen. Control (A) and blank hydrogel (B) groups show proliferative splenic (black arrow) changes with vascular congestion. The tail vein free drug (C) group exhibits disrupted splenic architecture with diffuse red pulp contraction (red rectangle), atrophied white pulp. In contrast, the intratumoral hydrogel-treated (D) group displays preserved splenic organization with clearly distinguishable red pulp and white pulp regions. **(E-H): Kidney.** Control (E) and blank hydrogel (F) groups show normal renal histology with few metastatic lesions (black arrow), intact glomeruli (white arrow) and well-organized renal tubules. The tail vein free drug group exhibits prominent renal injury, including tubular damage and cellular infiltration (black arrow). The intratumoral hydrogel-treated group shows preserved renal architecture with intact glomeruli and minimal histological abnormalities. Hematoxylin and eosin staining; scale bar = 50 μ m.

(Fig. 3A-D). In the control and blank hydrogel groups, the spleen showed features of high-grade lymphoid proliferation with advanced proliferative changes and vascular congestion, consistent with tumour burden-associated systemic involvement. In the tail vein free drug group, splenic architecture was severely disrupted, characterized by diffuse contraction of the red pulp, marked atrophy of the white pulp, and extensive cellular infiltration. These alterations indicate lymphoid depletion and loss of normal splenic organization. In contrast, the intratumoral hydrogel-treated group exhibited relatively preserved splenic architecture, with clearly distinguishable red pulp and white pulp regions and absence of major pathological abnormalities. The splenic alterations observed in the tail vein free drug group are consistent with chemotherapy-induced myelosuppression and immune compromise following prolonged systemic exposure to doxorubicin, paclitaxel, and cyclophosphamide, which are known to impair lymphoid tissue integrity and hematopoietic function (Hilbert-Carius et al., 2018). The preservation of splenic architecture in the intratumoral hydrogel group supports previous reports indicating that localized drug delivery reduces systemic immune toxicity and maintains lymphoid organ integrity.

Renal histopathological analysis showed normal kidney architecture (Fig. 3E-H) in the control and blank hydrogel groups, with intact glomeruli, well-organized renal tubules, and clearly defined cortical and medullary regions. Only minimal metastatic lesions associated with cellular infiltration were observed in these groups. In contrast, kidney sections from the tail vein free drug group demonstrated

evident signs of renal toxicity, including tubular dilation, epithelial desquamation, loss of brush border integrity, and possible glomerular shrinkage or vacuolation. These features indicate significant chemotherapy-induced renal injury. Importantly, kidneys from the intratumoral hydrogel-treated group displayed largely intact renal architecture, with normal-appearing glomeruli and tubules and no obvious signs of nephrotoxicity. The renal damage observed in the tail vein free drug group aligns with previously reported nephrotoxic effects of systemic cyclophosphamide and doxorubicin, which can impair both glomerular and tubular function following repeated exposure (Botros et al., 2024; Mohammed et al., 2025). In contrast, the absence of renal pathology in the intratumoral hydrogel group demonstrates that localized drug delivery minimizes renal drug exposure and significantly reduces chemotherapy-induced nephrotoxicity.

Histopathological examination of lung sections (Fig. 4A) revealed distinct treatment-dependent differences. In the control group, lung tissue exhibited densely packed cellular masses with marked distortion of normal alveolar architecture, consistent with extensive metastatic involvement. Similarly, the blank hydrogel group showed collapsed alveolar spaces, prominent cellular infiltration, and dense tumour cell aggregates, indicating progressive pulmonary metastasis and lack of therapeutic effect of the blank hydrogel. The metastatic lesions observed in the control and blank hydrogel groups were characterized by densely packed, pleomorphic tumour cells with hyperchromatic nuclei, high nuclear-to-cytoplasmic ratio, and loss of normal alveolar boundaries.

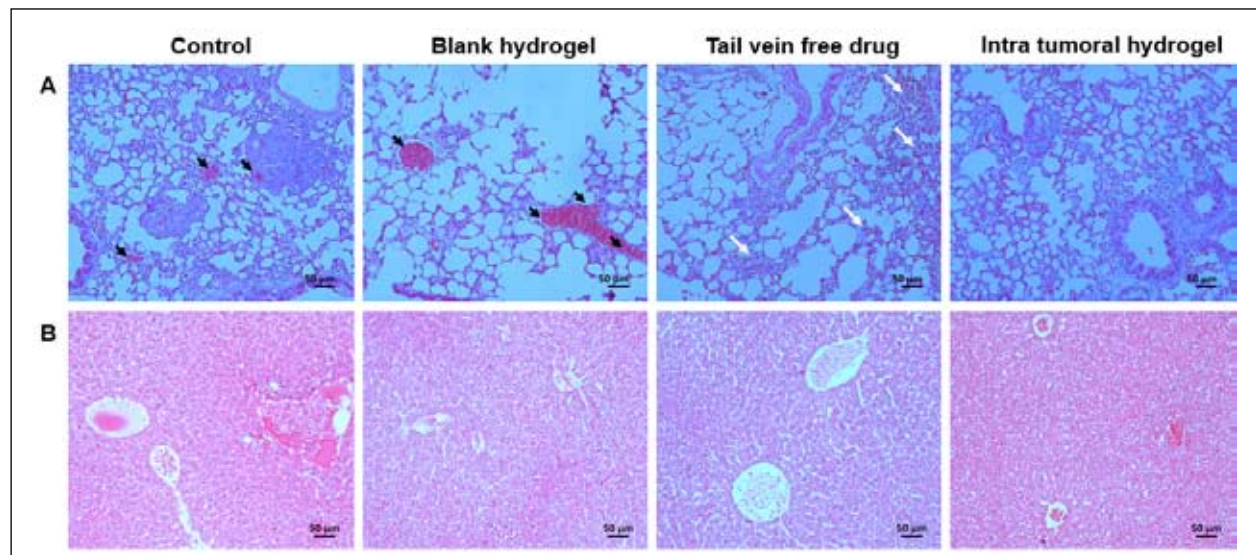


Fig. 4. Histopathological evaluation of lung and liver tissues

(A): Lung. Control and blank hydrogel groups show extensive metastatic lesions characterized by dense clusters of infiltrating tumour cells (black arrow) and distortion of normal alveolar architecture. The tail vein free drug group shows partial preservation of alveolar spaces with reduced cellular infiltration and focal fibrotic regions (white arrow). The intratumoral hydrogel-treated group demonstrates well-preserved alveolar architecture with minimal cellular infiltration, indicating effective suppression of pulmonary metastasis. **(B): Liver.** Liver sections from all experimental groups display preserved hepatic architecture with intact hepatic cords, central veins, and sinusoids, with no observable histopathological abnormalities. Hematoxylin and eosin staining; scale bar = 50 μ m.

These cells formed compact clusters replacing normal lung parenchyma, consistent with aggressive metastatic tumour infiltration. The tail vein free drug group demonstrated partial preservation of alveolar spaces with reduced cellular infiltration compared to control groups; however, focal fibrotic regions and residual cellular aggregates were observed, suggesting limited suppression of metastatic spread along with possible chemotherapy-induced tissue response. In contrast, the intratumoral hydrogel-treated group displayed well-preserved alveolar architecture with open air spaces and minimal cellular infiltration, indicating effective suppression of pulmonary metastasis and reduced lung toxicity following localized drug delivery. The extensive lung metastasis observed in the control and blank hydrogel groups aligns with earlier reports of unchecked tumour dissemination in the absence of effective therapy (Yu et al., 2023). Partial improvement in the free drug group is consistent with systemic chemotherapy reducing tumour burden but inducing tissue stress. The marked preservation of lung architecture in the intratumoral hydrogel group supports previous studies demonstrating that localized drug delivery limits metastatic spread while minimizing pulmonary toxicity.

Histological examination of liver sections (Fig. 4B) revealed preserved hepatic architecture across all experimental groups. The control, blank hydrogel, tail vein free drug, and intratumoral hydrogel groups exhibited well-organized hepatic cords, intact central veins, and normal sinusoidal spaces, with no evidence of hepatocellular degeneration, inflammatory infiltration, or necrosis. The absence of histopathological alterations in liver tissue across all groups is consistent with previous reports indicating relative hepatic tolerance to the administered chemotherapeutic regimens at the studied doses (Sharma et al., 2014). These findings further suggest that neither systemic nor intratumoral delivery of the drug combination induced detectable liver toxicity under the experimental conditions.

These findings suggest that localized intratumoral delivery via intra tumoral hydrogel group offers a significant advantage by reducing systemic exposure, limiting metastatic progression, and minimizing organ toxicity when compared to prolonged systemic free drug administration. Overall, these observations confirm that intra tumoral hydrogel treatment offers superior protection of non-target organs, preserves normal tissue integrity, and avoids the off-target toxicity typically associated with prolonged systemic chemotherapy.

Conclusion

In conclusion, the intra tumoral hydrogel group showed well-preserved morphology in all major organs, minimal systemic toxicity, and protection against metastatic spread. In conclusion this study demonstrates that a single intra-tumoral injection of intra tumoral hydrogel reduces

systemic drug burden, preserves healthy organ histology, and limits metastatic dissemination compared to repeated systemic chemotherapy. This localized drug delivery platform shows great promise for safer and more effective TNBC therapy.

Acknowledgments

We wish to thank University Grants Commission (UGC), New Delhi for providing Junior Research Fellowship to Lenkapothena Naresh Goud and Department of Biotechnology (DBT) for funding. The authors gratefully acknowledge Dr. Archana S, Animal Research Facility, RGCB, Thiruvananthapuram, India, for her support in all animal experiments.

Conflict of interest

There are no conflicts of interest reported by the authors.

References

- Botros SR, Matouk AI, Amin A and Heeba GH (2024). Comparative effects of incretin-based therapy on doxorubicin-induced nephrotoxicity in rats: the role of SIRT1/Nrf2/NF- κ B/TNF- α signaling pathways. *Front. Pharmacol.* 15, 1353029.
- Bruna J, Alberti P, Calls-Cobos A, Caillaud M, Damaj MI and Navarro X (2020). Methods for in vivo studies in rodents of chemotherapy-induced peripheral neuropathy. *Exp. Neurol.* 325, 113154.
- Cardiff RD, Miller CH and Munn RJ (2014). Manual hematoxylin and eosin staining of mouse tissue sections. *Cold Spring Harbor Protocols* 2014(6), 655–658.
- Chen L, Sun X, Wang Z, Chen M, He Y, Zhang H, Han D and Zheng L (2024). Resveratrol protects against doxorubicin-induced cardiotoxicity by attenuating ferroptosis through modulating the MAPK signaling pathway. *Toxicol. Appl. Pharmacol.* 482, 116794.
- Florescu M, Cinteza M and Vinereanu D (2013). Chemotherapy-induced cardiotoxicity. *Maedica (Bucur.)* 8, 59–67.
- Hilbert-Carius P, Kaden I, Berg T and Weigert N (2018). A rare cause of splenomegaly. *Dtsch. Arztbl. Int.* 115, 116.
- Lehmann HC, Staff NP and Hoke A (2020). Modeling chemotherapy-induced peripheral neuropathy (CIPN) in vitro: prospects and limitations. *Exp. Neurol.* 326, 113140.
- Mohammed Hegab AM, Hassanin SO, Mekky RH,

Abuzahrah SS, Hamza AA, Talaat IM and Amin A (2025). *Withania somnifera* ameliorates doxorubicin-induced nephrotoxicity and potentiates its therapeutic efficacy targeting SIRT1/Nrf2, oxidative stress, inflammation, and apoptosis. *Pharmaceutics* 18, 248.

Myung N and Kang H-W (2024). Local dose-dense chemotherapy for triple-negative breast cancer via minimally invasive implantation of 3D-printed devices. *Asian J. Pharm. Sci.* 19(1), 100884.

Radswiki T, Campos A, Yap J and others (2025). Radiation and chemotherapy induced cystitis. *Radiopaedia*.

Ritchey M, Ferrer F, Shearer P and Spunt SL (2009). Late effects on the urinary bladder in patients treated for cancer in childhood: a report from the Children's Oncology Group. *Pediatr. Blood Cancer* 52, 439–446.

Sharma A, Houshyar R, Bhosale P, Choi JI, Gulati R and Lall C (2014). Chemotherapy-induced liver abnormalities: an imaging perspective. *Clin. Mol.* *Hepatol.* 20, 317–326.

Spears N, Lopes F, Stefansdottir A, Rossi V, De Felici M, Anderson RA and Klinger FG (2019). Ovarian damage from chemotherapy and current approaches to its protection. *Hum. Reprod. Update* 25, 673–693.

Sung H, Ferlay J, Siegel RL, Laversanne M, Soerjomataram I, Jemal A and Bray F (2021). Global Cancer Statistics 2020: GLOBOCAN Estimates of Incidence and Mortality Worldwide for 36 Cancers in 185 Countries. *CA Cancer J. Clin.* 71, 209–249.

Yu J, Xie X, Wang L, Liu W, Xu H, Lu X, Li X, Ren J and Li W (2023). Smart chondroitin sulfate micelles for effective targeted delivery of doxorubicin against breast cancer metastasis. *Int. J. Nanomed.* 18, 663–677.

Zagami P and Carey LA (2022). Triple negative breast cancer: pitfalls and progress. *npj Breast Cancer* 8, 95. ■